

**THE NONLINEAR AND NONSTATIONARY  
PROPERTIES IN EEG SIGNALS: PROBING  
THE COMPLEX FLUCTUATIONS  
BY HILBERT–HUANG TRANSFORM**

MEN-TZUNG LO\*, PING-HUANG TSAI<sup>†,‡,§</sup>, PEI-FENG LIN<sup>¶,||</sup>,  
CHEN LIN<sup>\*,\*\*</sup> and YUE LOONG HSIN<sup>††</sup>

*\*Research Center for Adaptive Data Analysis  
National Central University, Chungli, Taiwan, ROC*

*†Neurology Department  
National Yang-Ming University Hospital, Yi-Lan, Taiwan, ROC*

*‡Graduate Institute of Biomedical Electronics and Bioinformatics  
National Taiwan University, Taiwan, ROC*

*§National Yang-Ming University School of Medicine  
Taipei, Taiwan, ROC*

*¶Graduate Institute of Clinical Medicine  
College of Medicine, National Taiwan University, Taiwan, ROC*

*||Department of Health, Executive Yuan  
Tainan Hospital, Tainan, Taiwan, ROC*

*\*\*Institute of Systems Biology and Bioinformatics  
National Central University, Taoyuan, Taiwan, ROC*

*††Neurology, Buddhist Tzu Chi General Hospital, Hualein, Taiwan, ROC*

The analysis of biological fluctuations provides an excellent route to probe the underlying mechanisms in maintaining internal homeostasis of the body, especially under the challenges of the ever-changing environment or disease processes. However, the features of nonlinearity and nonstationarity in physiological time series limit the reliability of the conventional analysis. Hilbert–Huang transform (HHT), based on nonlinear theory, is an innovative approach to extract the dynamic information at different time scales, in particular, from nonstationary signals. In this paper, HHT is introduced to analyze the alpha waves of human’s electroencephalography (EEG), which seemly oscillate regularly between 8 and 12 Hz in healthy subject but getting irregular or disappeared in different demented status. Furthermore, conventional time–frequency analyses are adopted to colate the results from those methods and HHT. Finally, the potential usages of HHT are demonstrated in characterizing the biological signals qualitatively and quantitatively, including stationarity analysis, instantaneous frequency and amplitude modulation or correlation analysis. Such applications on EEG have successively disclosed the differences of alpha rhythms between normal and demented brains and the nonlinear characteristics of the underlying mechanisms. Hopefully, in addition to empower the studies of EEG

\*Corresponding author.

varied in diseased, aging, and physiological processes, these methods might find other applications in EEG analysis.

*Keywords:* Nonstationary; nonlinear; EEG; dementia; Hilbert–Huang transform; coherence; brain topography; intrawave frequency modulation; interwave frequency; time frequency analysis.

## 1. Introduction

The surface electroencephalopathy (EEG) has been widely used in clinical practice for decades. Different brain waves that EEG depicts are the temporal and spatial summations of interacted neuronal potentials postsynaptically. The changes of brain waves reflect the information processing of central nervous system. Even though there is significant progress in the development of neuroimages for the diagnosis of neurological disorders and the evaluation of brain function, the EEG, a noninvasive, portable and inexpensive tool, remains its leading role in the assessment of dynamic brain activities.

EEG signals are composed of multiple oscillation components. The mechanism is still unclear though, four conventional bands, delta (0.5–4 Hz), theta (4–8 Hz), alpha (8–12 Hz), and beta (12–25 Hz) rhythms, were categorized since Hans Berger (1924). There has been a tremendous amount of researches working on the clinical significance of individual frequency bands, based on their locations, amplitudes, and frequency shifts.<sup>1–5</sup> In recent years, with digitalized signals, many quantitative EEG (qEEG) methods were developed, including topography displays, the software of automatic detection and localization of epileptic discharges, and the statistical analysis comparing data to the norm. Through the development of quantitative EEG, clinicians are trying to expand the use of EEG. In these methods, spectral analysis, which easily extracts the EEG signals into the four main frequency bands, has become one of the most commonly used objective tools for characterizing the alternation of EEG from one state to another and the significant abnormalities.

Numerous neurological and psychiatric disorders were evaluated by qEEG, focusing on the alpha rhythms.<sup>3–5</sup> According to many animal models, the origins of alpha rhythms may include a complex interaction between the lateral geniculate body, the thalamus and the cortex and is thought to represent the level of consciousness and cognitive function.<sup>6</sup> Previous studies have also confirmed that the power of the alpha rhythms decreases with age and the severity of dementia.<sup>4</sup> However, in these studies, only very severe disorders could be distinguished from the normal subjects.<sup>3,4</sup> Although the amplitude of EEG signals is related to the degree of pathology- or age-related degenerations, there is little clinical use. Because it is highly affected by boundaries like thickness of the dura matter, the skull, the scalp, and the amount of cerebrospinal fluid.<sup>7</sup> On the other hand, all the traditional spectral analyses of qEEG are based on Fourier transform, which assume that the signals are composed of superimposed sinusoidal oscillations of constant amplitudes

and periods at a pre-determined frequency range. This assumption puts an unavoidable limitation on the reliability and the applicability of the method. Since EEG represents the output of the interactions between neural networks, it is not necessarily linear. Many deterministic chaos-based methods are applied to characterize the embedded intrinsic nonlinearity of EEG signals.<sup>8–11</sup> However, most of these methods need a critical condition that the time series should be stationary.<sup>12–14</sup> Such constraint unfortunately makes conventional approaches unreliable in the analysis of physiological signals, since the nonstationarity (i.e. statistical properties such as mean and standard deviation vary with time) is an intrinsic feature of physiological data and it persists even without external intervention.<sup>15</sup> To solve the difficulties related to nonlinearity and nonstationarity, one of the innovative approaches is Hilbert–Huang transform (HHT).<sup>16</sup> The HHT is based on nonlinear theories and has been designed to extract dynamic information from nonstationary signals at different time scales. The advantages of the HHT over traditional Fourier-based methods have been appreciated in many studies of different physiological systems such as blood pressure hemodynamics,<sup>17</sup> cerebral autoregulation,<sup>18–22</sup> cardiac dynamics,<sup>23</sup> respiratory dynamics,<sup>24</sup> and electroencephalographic activities.<sup>25</sup> In this study, we examined how HHT can profile the nonlinear and nonstationary characteristics of human alpha waves, and compared the performances of HHT with conventional methods in analyzing EEG fluctuations. We aimed to extract certain features from HHT spectrum, which may be a potential noninvasive tool for the diagnosis of neuronal disorders.

## **2. Materials**

EEGs were recorded in all subjects as part of the examination protocol. According to the IFCN standards for digital recording of the clinical EEG,<sup>26</sup> the surface EEG signals were recorded by the digital EEG recorder (NicoletOne), from the 19 scalp loci of the international 10–20 system (channels Fp1, Fp2, F3, F4, C3, C4, P3, P4, O1, O2, F7, F8, T3, T4, T5, T6, Fz, Cz, and Pz), with all electrodes referenced to the bilateral ear (A1, A2) for 30 min. Electrocardiogram (ECG) was recorded in a separate channel. Sample frequency is 256 Hz and A/D digitalized resolution is 12 bits. Alpha rhythms are believed to appear most prominently when people close their eyes with awareness and relaxation. Therefore, all subjects in this study were arranged to get 30 min of eye-closed EEG, from which 30 s of signals without artifact are selected by an experienced neurologist. The data was copied as comma separated value (CSV) file without any filter. In this study, we attempt to specify the alterations of alpha waves in neuronal disorders. Three subjects were included, one healthy control and two patients from the neurological outpatient department in National Yang Ming University Hospital. One patient is with mild dementia of Alzheimer's type (mini-mental status examination (MMSE) = 26, Clinical rating scale (CDR) = 1) and the other is in the late stage of the same disease, almost in deep comatose state (MMSE = 0 and CDR = 5).

### 3. Methods — Hilbert–Huang Transform

The HHT algorithms require two steps in analyzing data. The first step is to preprocess the data by the empirical mode decomposition (EMD) algorithm.<sup>16</sup> The decomposition is based on the simple assumption that any data consists of a finite number of intrinsic modes of oscillations. The first mode is obtained by tracing the envelope of local maxima and local minima of the repetitive signal. The first mode is then subtracted from the original signal to obtain the first residual signal. The second mode is obtained by tracing the envelope of the maxima and minima in the first residual signal. The subsequent modes of oscillations, termed intrinsic mode functions (IMFs), are decomposed from the residual signals of the previous one following the same procedure. Each IMF represents a certain frequency–amplitude modulation at a specific time scale, and therefore it can be used to analyze temporal or phase associations with comparable IMFs from other signals. For signals with intermittent oscillations, one essential problem in the EMD is that an intrinsic mode could comprise oscillations with very different wavelengths at different temporal locations (i.e. mode mixing). The problem can cause certain complications for our analysis, making the results less reliable. To overcome the mode mixing problem, a noise assisted EMD algorithm, namely the ensemble empirical mode decomposition (EEMD) has been proposed.<sup>27,28</sup> The EEMD applies the EMD to obtain an ensemble of decompositions of data with added white noise, and uses the resultant means of the corresponding intrinsic mode functions from different decompositions as the final result. The second step is to apply the Hilbert transform to the decomposed IMFs and construct the energy–frequency–time distribution, designated as the Hilbert spectrum. The biological fluctuations are not stationary and are better characterized by analytical methods that can quantify the amplitude and phase/frequency from time to time.<sup>29–31</sup> Hilbert transform provides a more informative and accurate tool to examine the nonlinear relationship between nonstationary signals.<sup>19–22</sup> Unlike the Fourier transform, the Hilbert transform does not assume that signals are composed of superimposed sinusoidal oscillations of constant amplitude and frequency. It provides the instantaneous amplitude and phase of an oscillation instead. Physically, the necessities to define a meaningful instantaneous frequency/phase are that the functions are symmetric with respect to the local zero mean and have the same numbers of zero crossings and extrema. The intrinsic mode function derived from empirical mode decomposed method satisfies the above conditions, since it holds the properties that (i) the total numbers of extrema and zeros crossings must either equal or differ at most by one and (ii) at any point, the mean value of the envelop defined by the local maxima and the local minima is zero. Thus, we can explore the instantaneous frequency and energy, rather than the global frequency and energy defined by the Fourier spectral analysis. These properties of the HHT make it ideal for quantitative and even qualitative analysis of complex biomedical signals.

## 4. Results

### 4.1. Stationarity of temporal–spectral distribution

As alpha rhythms are best seen in the occipital region of the brain, in this study, signals at an occipital electrode (i.e. O1) will be examined at first. Figure 1 gives the raw O1 EEG signals recorded from three different subjects, who are normal control, mildly demented, and severe demented in deep coma. The investigation of raw data shows several facts that are (i) the EEG signals of the normal and the mildly demented subjects oscillate more quickly than that of the one in deep coma. (ii) The EEG morphologies of the normal and the mildly demented subjects look similar, difficult to distinguish one from the other by visual inspection. (iii) Sinusoidal wavelets appear intermittently rather than consistently in the EEG signals of the normal and the mildly demented subjects. Some of the above observations may be quantified by the linear Fourier analysis; however, the characteristics in visual inspection including irregular morphologies and intermittent/nonstationary sinusoidal wavelets could not be understood well by the Fourier spectra. Therefore, we propose some novel methods based on HHT to quantify such nonlinear and nonstationary characteristics of EEG signals.

In order to study the nonstationary characteristic of brain waves, time–frequency analyses are applied to the signals from different subjects, and we give the results of the normal control, the mild dementia, and the deep coma as shown in Fig. 2. Two conventional time frequency analyses including short-time Fourier transform (STFT) and continuous Morlet wavelet transform<sup>32</sup> are adopted to compare with the novel HHT. Each analysis shows a significant power in the frequency range of 8–12 Hz (i.e the alpha rhythms) in the normal control, and the mild dementia, while significantly reduced in the subject in deep coma. This agrees with the discovered fact that the appearance of alpha rhythm is an indicator of awareness.<sup>33</sup>

The study of the temporal frequency that features from the results of STFT analysis shows concentrated energetic frequencies with no fluctuation over time in both normal control and the mildly demented subjects, which consequently leads to a misunderstanding that alpha rhythms in these two subjects are of consistent sinusoidal function. On the contrary, using the continuous Morlet-wavelet and the HHT, the frequency distributions fluctuate moderately with time in the normal control, and even more wildly in the mildly demented subject. In addition, the power of alpha rhythm frequencies are not consistent over time. Obviously, many intermittent drops can be observed in both continuous Morlet-wavelet and Hilbert–Huang spectrums. Accordingly, the temporal frequency features from Morlet-wavelet and HHT analyses reveals that the “alpha rhythms” are not of pure sinusoidal functions, or rather, they are more similar to the combinations of many sinusoidal wavelets with varied amplitude and wavelength, which are stitched together one by one.

We have demonstrated that the dominant frequency distribution in Hilbert–Huang spectrum varies with time, and in order to measure this inconsistency, two

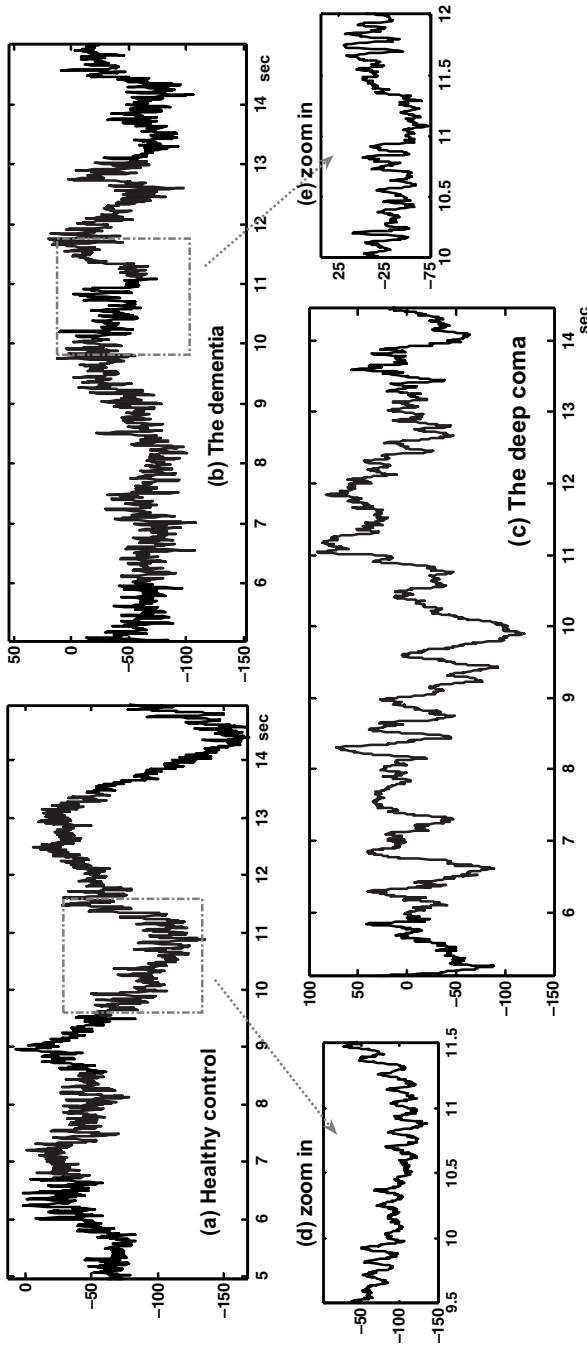


Fig. 1. The comparison of EEG time domain signals recorded from three different subjects, who are (a) normal control, (b) mildly demented, and (c) severe demented in deep coma. We zoom in the time domain signals over 9.5–11.5 s for normal subject and over 10–12 s for mildly demented one and plot the details in (e) and (f).

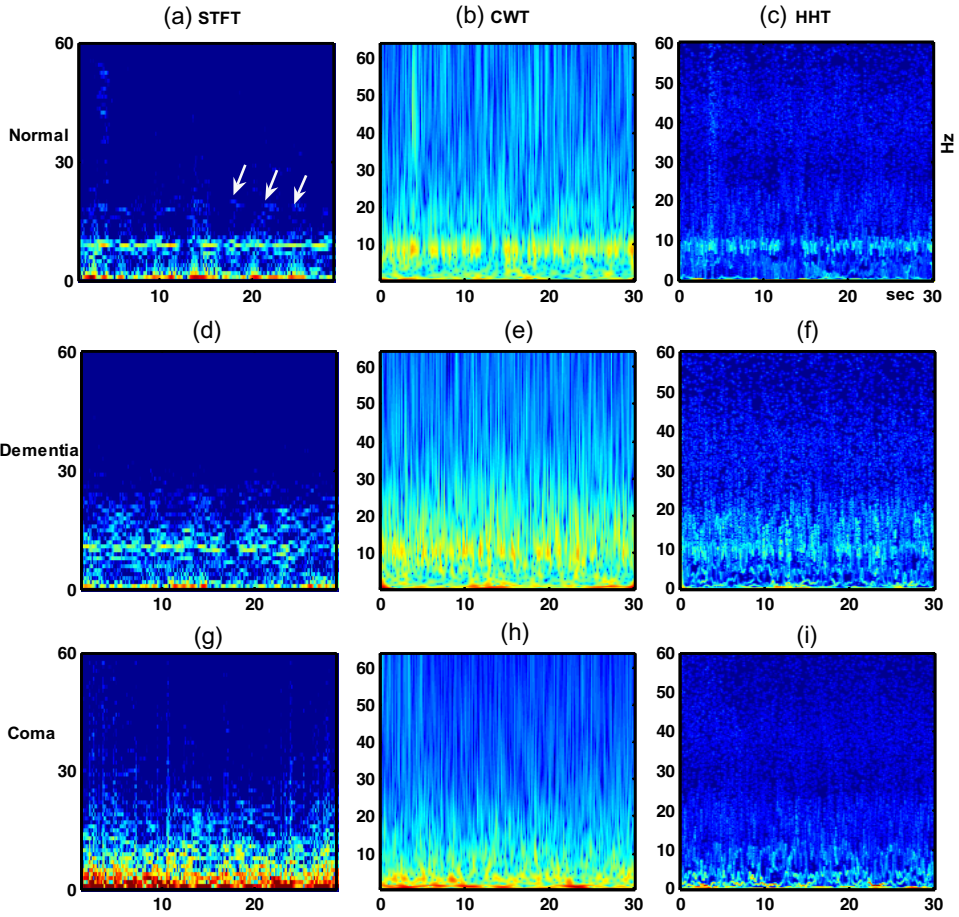


Fig. 2. The comparison of the results between conventional time frequency analysis including short-time Fourier transform (STFT) and continuous Morlet wavelet transform, and the novel Hilbert–Huang transform from normal control (a–c), mildly demented subjects (d–f), and severe demented subject in deep coma (g–i).

quantitative methods named “degree of stationarity”,<sup>16</sup> developed by Huang *et al.*, and its extended method named “Shannon entropy of marginal spectrum” recently established by Tong *et al.*,<sup>34</sup> are introduced in this study. Degree of stationarity (DS), conceptually indicating the average deviation of frequency response over time from the mean marginal spectrum is given as

$$DS(w) = \frac{1}{T} \int_0^T \left( 1 - \frac{H(w, t)}{n(w)} \right)^2 dt, \quad (1)$$

where  $H(w, t)$  is the Hilbert spectrum of IMFs from EEMD except unwanted trends and  $n(w)$  is the mean marginal spectrum, defined as  $\frac{1}{T} \int_0^T H(w, t) dt$ . Different from the classic definition of stationarity,<sup>35</sup> which gives only the qualitative description

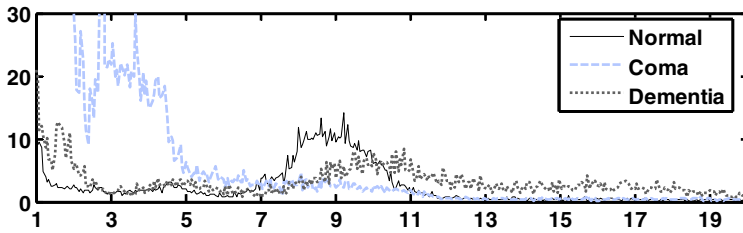
for the stochastic process, DS provides a quantitative index of stationarity for specific spectral components. According to Eq. (1), when the energy of the frequency,  $w_i$  is invariant with time, that is  $H(w_i, t) \approx n(w_i)$ , apparently,  $DS(w_i)$  will be close to zero. On the contrary, the DS will become larger as the energy distribution of  $w_i$  diverse over time.

Shannon entropy of marginal spectrum (SE) is an entropy-based measurement, also powerful at the quantification of the stationarity for specific frequencies in Hilbert–Huang spectrum like DS. Shannon entropy of marginal spectrum, which is ideally used to measure how uniform the distribution of the power for specific frequencies over time would be, is given as

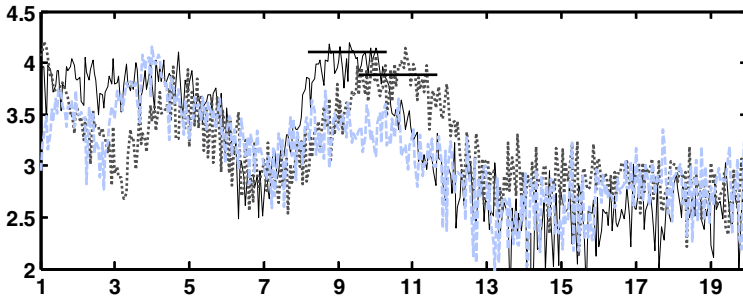
$$SE(w) = - \int \frac{H(w, t)}{n(w) \cdot T} \cdot \log \left( \frac{H(w, t)}{n(w) \cdot T} \right) dt. \quad (2)$$

According to Eq. (2), the SE will approach to its maximum value when the power for specific frequencies has a uniform distribution over time, and the SE for such frequencies will degrade substantially once these frequency components appear occasionally during recording, thus the larger SE indicates higher stationarity.

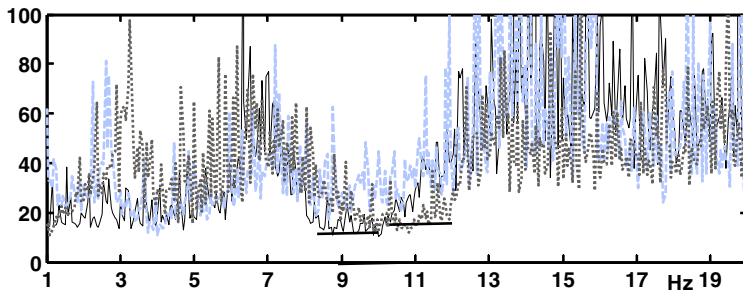
The marginal spectrum, SE, and DS for three subjects are given in Fig. 3 from the top to the bottom panels. Note that the marginal spectrum is also used to indicate the constitutive frequency components of time series, nevertheless it is quite different from the Fourier spectrum. It can avoid including some broadened frequency components due to windowing effects.<sup>36</sup> For instance, a time series with zero value for the whole time but one sinusoidal wavelet localized at the center of the time series has a very narrow frequency distribution in the marginal spectrum in comparison with Fourier spectrum. Accordingly, the marginal spectrum provides more precision in studying the frequency components for intrinsically nonstationary signals. According to the marginal spectrum for the normal control, the substantial intensity of spectrum can only be observed within a specific frequency range (7.5–11.5 Hz), while for the mildly demented patient, high intensities of spectrum are shown in several frequency ranges such as 1–3, 3–7, and 9–19 Hz. We compared the mean values of the DS and the SE in the frequency range of 8.5–10.5 Hz for the normal subject with that in the frequency range of 9.5–11.5 Hz for the mildly demented subject, and found that the DS is smaller (Fig. 3(c)) and the SE is larger (Fig. 3(b)) in the normal control. This shows that although the alpha rhythm frequencies in both cases exhibit significant high energy in the marginal spectrum, the stationarities of the two datasets are different, as the alpha rhythms of the normal subject seem more stationary than that of the mildly demented patient. Different from the other two cases, the marginal spectrum for the patient in deep coma shows no significant intensity in the frequency band related to alpha rhythms. In the case of mildly demented patient, besides the alpha rhythms, the oscillations with frequencies over 13 Hz have rather high intensity in the marginal spectrum with large DS and small SE measurements. It shows that such oscillations are only intermittently, not consistently exhibited in the whole recording in spite of the



(a) marginal spectrum



(b) SE



(c) DS

Fig. 3. From the top to the bottom panels, there are (a) the marginal spectrum, (b) frequency function of SE, and (c) frequency function of DS for the three subjects who are normal control (solid line), mildly demented (gray dotted line), and severe demented in deep coma (gray dashed line).

substantial power in frequency response. As to the other prominent slow oscillations with frequencies of 3–7 Hz, the corresponding intensity in the marginal spectrum is almost equal to that in high frequencies (13–19 Hz), however, the slow oscillations are quite stationary since the values of the DS and the SE are at the same degree as the alpha rhythms’.

The conventional visual findings of EEGs in Alzheimer’s disease (AD) reveal the slowing of the dominant posterior rhythms as well as the reduction in the alpha

activities.<sup>3,5</sup> In this study, the energetic frequencies of the mildly demented patient do not shift downwards compared with the normal subject, which might fail to express the slowing of EEG. However, recent clinical reports show that the slowing of the alpha rhythms are prominent in severe demented patients, but rarely seen in mild cases.<sup>3,4</sup> In other words, the mildly demented patients do not necessarily exhibit the slowing of EEG. As a consequence, it limits the application of spectral analysis of EEG in the diagnosis of early stage dementia.

On the other hand, conventional clinical studies have also reported an increase of diffuse slow (delta and theta) activities in AD patients.<sup>37–39</sup> According to the marginal spectrum in this study, the EEG signal recorded from the demented patient is not as monotonic as the normal subject; rather it consists of multiple frequency components, thus heightening the ratios of other waves to the alpha waves. The stationary tests give further evidence that the occurrence of slow oscillations (delta and theta waves) in demented patients are not intermittent, actually that are pretty consistent.

According to some animal studies, a much wider dominant frequency range, theta rhythms (3–12 Hz), generated from the hippocampus of lower mammals, are thought to be the equivalent of both alpha (8–12 Hz) plus theta (4–8 Hz) waves in human EEG.<sup>40</sup> Some hypothesis suggested that the development of the alpha rhythms results from the complex interactions between the cortical neurons in the highly developed cortex of the human brain; the sum of the synchronization of the postsynaptic potentials of these highly developed cortical neurons are the alpha waves.<sup>4</sup> We suppose that as people become demented, the complicated interaction between cortical neurons become less synchronized, therefore the power of the alpha rhythms decreases and that of the theta rhythms increases as the inhibition from alpha to theta decreases. Our study may provide an alternative way to evaluate the relationship between the alpha and the theta rhythms. Do the alpha and the theta rhythms come from different sources of the EEG, or do they come from the same origin but representing different degrees of the synchronization of the neurons?

#### 4.1.1. *Intrawave and interwave frequency modulations*

Although the marginal spectrum of EEG signals shows that the intensity is concentrated in limited frequency range, the EEG signals are visually irregular in waveform. Thus, it would be better to treat the EEG fluctuations as the output of nonlinear system. The Fourier analysis traditionally can also be used to characterize the nonlinearity of signal by its harmonic components. For example, a sinusoidal oscillation with sharp crests and rounded-off troughs exhibits higher harmonics in the Fourier spectrum, which is because the Fourier analysis needs higher harmonics to reconstruct the waveform deviation from sinusoidal wave caused by nonlinear effects, even though the true signal contains no waves with half or one-third period of the fundamental one. The appearance of those harmonics provides a qualitative indicator for the nonlinearity of the signal, though it lacks physical meanings. Thus

it could not afford to resolve the complicated frequency modulation from a nonlinear system. The nonlinear harmonics related to the waveform distortion can also be shown in the EEG signals by STFT for the normal control (see white arrow mark in Fig. 2(a)), while it is not clear in the mildly demented and the comatose patients.

Instead of investigation of harmonics, Huang *et al.*<sup>16</sup> proposed a novel insight to profile the nonlinear dynamics by frequency modulation. For instance, a modeling wave which satisfies the following nonlinear differential equation,

$$\frac{d^2x}{dt^2} + (w + \varepsilon w \cos wt)^2 - \varepsilon w^2 \sin wt(1 - x^2)^{1/2} = 0 \quad (3)$$

is given by

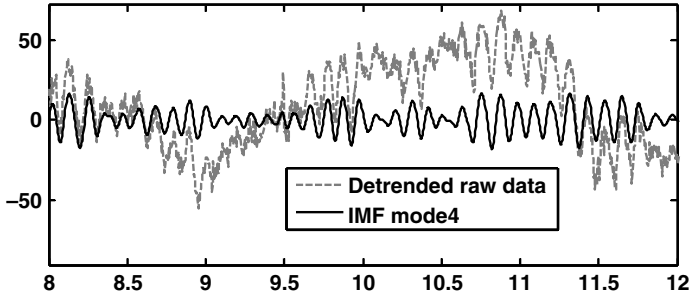
$$x(t) = \cos(wt + \varepsilon \sin wt). \quad (4)$$

The modeling wave can be approximated as the linear combination of weighted fundamental and harmonic components mathematically in Fourier analysis, that is,

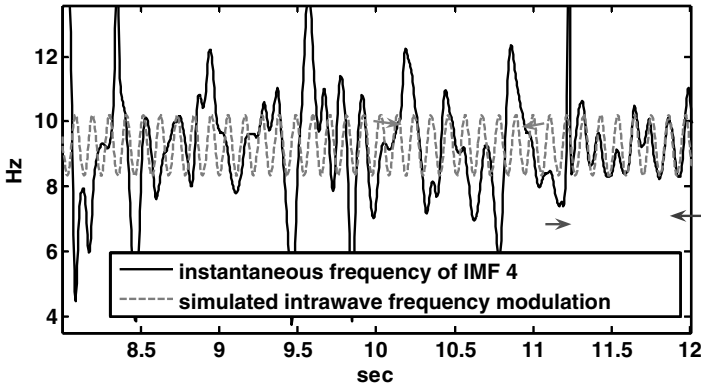
$$x(t) \approx \left(1 - \frac{1}{2}\varepsilon\right) \cos wt + \frac{1}{2}\varepsilon \cos 2wt. \quad (5)$$

By contrast, the HHT can derive the instantaneous frequency, which is much similar to the analytic solution, i.e. the frequency of such wave will oscillate periodically over time around the mean frequency denoted as  $w$ . Such phenomenon named as intrawave frequency modulation gives a more physical interpretation for the nonlinear alternation in the waveform. Huang *et al.*<sup>16</sup> has shown various types of intrawave frequency modulations in the oscillations driven from several classic nonlinear dynamic equations such as Duffing, Lorenz, and Rössler equations while the Fourier analysis can only provide similar display of harmonics distribution.

To illustrate the frequency modulation caused by nonlinearity, we give the instantaneous frequency of the IMF mode 4 for the normal control in Fig. 4(b). The IMF mode 4 is regarded as the oscillation of the alpha rhythms with the criterion that the IMF mode 4 has the maximum power than other modes within the frequency range of 8–13 Hz. The comparison of the detrended EEG raw data and the IMF mode 4 is demonstrated in Fig. 4(a) showing that the IMF mode 4 keeps almost the same morphology as the raw data. To specify whether the intrawave frequency modulation occurs in the EEG signal, the simulated time function of instantaneous frequency for Eq. (4) is plotted in Fig. 4(b), where  $w$  is given as the median value of the instantaneous frequency over time from 8 to 12 s, and  $\varepsilon$  is set at 0.2. It can be found that the instantaneous frequency of the IMF mode 4 coincides with simulated result over time from 11–12 s. However, the instantaneous frequency, except for the epoch of 11–12 s, does not oscillate periodically and has smoother but larger fluctuations, indicating that the oscillations of the IMF mode 4 at that time are subject to interwave frequency modulation, i.e. each wave in the oscillations has a time variant duration. Accordingly, we have observed both



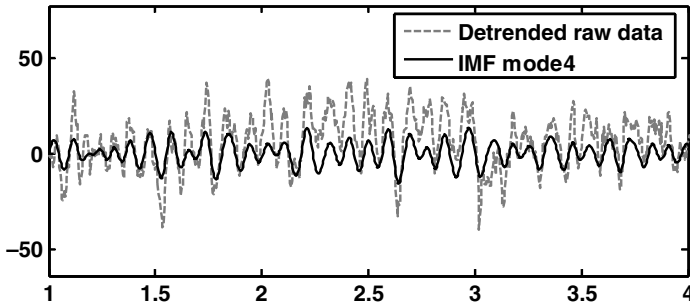
(a)



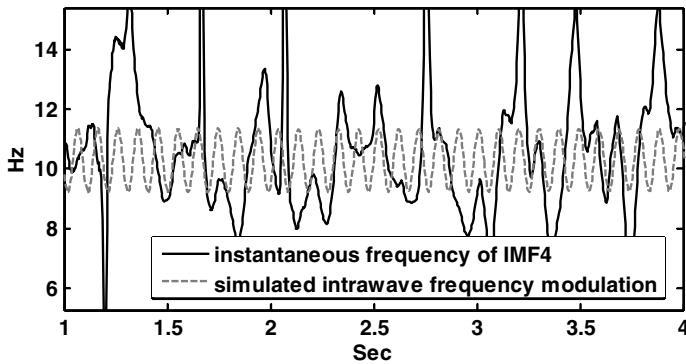
(b)

Fig. 4. (a) The comparison of the detrended EEG raw data (gray dashed line) and the IMF mode 4 (solid line) for normal control subject. (b) The comparison of instantaneous frequency of the IMF mode 4 (solid line) from normal control subject and simulated time function of instantaneous frequency related to intrawave frequency modulation as Eq. (4) (gray dashed line), where  $w$  is given as the median value of the instantaneous frequency over time ranging from 8 to 12 s, and  $\varepsilon$  is set at 0.2.

intrawave and interwave frequency modulations simultaneously in the EEG signals from the normal control. Following the same procedure, the corresponding results for the mildly demented patient are given in Fig. 5. However, it is hard to find any intrawave frequency modulation in the IMF mode 4 in this patient. The histograms of the instantaneous frequencies related to alpha rhythms (i.e. IMF mode 4) for all the three subjects are given in Fig. 6(a), and the corresponding ratios of the standard deviations to the mean values of the instantaneous frequency distributions are illustrated in Fig. 6(b). Clearly, the instantaneous frequency of the IMF mode 4 for the normal control has fewer fluctuations over time, resulting in highly concentrated distribution in the corresponding histogram. We have shown that the fluctuations of instantaneous frequency for the normal control are contributed from both the intrawave and interwave frequency modulations, nevertheless the two modulations



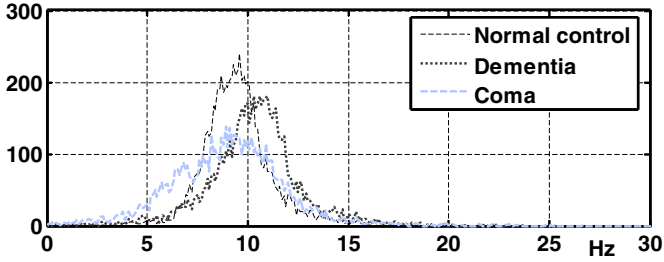
(a)



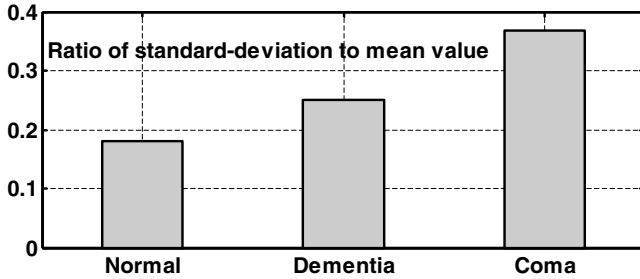
(b)

Fig. 5. (a) The comparison of the detrended EEG raw data (gray dashed line) and the IMF mode 4 (solid line) for mildly demented subject. (b) The comparison of instantaneous frequency of the IMF mode 4 (solid line) from mildly demented subject and simulated time function of instantaneous frequency subject to intrawave frequency modulation as Eq. (4) (gray dashed line), where  $w$  is given as the median value of the instantaneous frequency over time ranging from 8 to 12 s, and  $\varepsilon$  is set at 0.2.

have different physical meanings and influence on the total fluctuations. The oscillation exhibiting intrawave frequency modulation actually has constitutive wavelets with constant wavelength; on the contrary, constitutive wavelets under interwave frequency modulation have diverse wavelengths. Inspection of the distribution of the instantaneous frequency of the IMF mode 4 for the normal control reveals less deviations under intrawave frequency, thus most of the deviations are contributed from interwave frequency modulation. Relative to the two demented patients, we have demonstrated weak fluctuations in the instantaneous frequency of the alpha rhythm oscillations in the normal subject. Therefore, the normal alpha rhythms can be modeled more evidently as the output of a nonlinear system with the appearance of intrawave frequency modulation; nevertheless, the normal alpha rhythms do not look very chaotic.



(a) The histogram of instantaneous frequency



(b)

Fig. 6. (a) The histograms of the instantaneous frequency for all three subjects who are normal control (solid line), mildly demented (gray dotted line), and severe demented in deep coma (gray dashed line). (b) The corresponding ratios of the standard deviations to the mean values of the instantaneous frequency distributions.

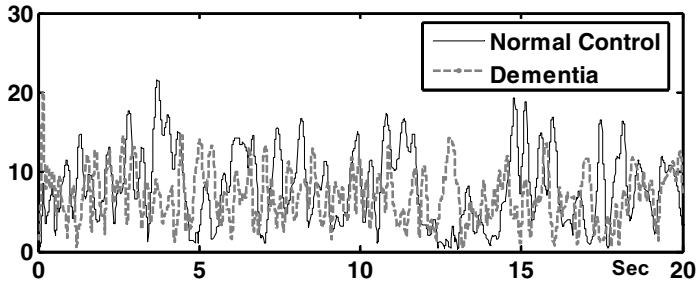
4.1.2. Continuity in instantaneous amplitude

The Hilbert transform provides both the frequency and the amplitude as function of time. As we have examined the frequency distribution of the extracted alpha rhythms over time in the previous section, the continuity of the instantaneous frequency in normal alpha rhythms have been found but failed to identify in neurological disorders such as dementia. In the section, we will specify whether the continuity is also exhibited in the other time function (i.e. the instantaneous amplitude).

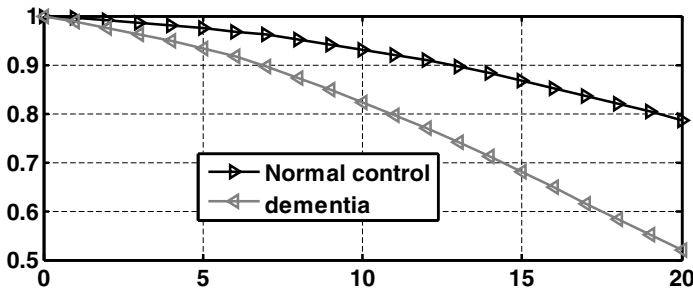
Figure 7(a) demonstrates the time functions of the instantaneous amplitude of the IMF mode 4 for the normal and the mildly demented subjects. From visual inspection, it seems that the normal alpha rhythms can sustain in evident amplitudes for longer durations. Using the classic autocorrelation function, i.e.

$$R(k) = \frac{1}{(n - k)\sigma^2} \sum_{t=1}^{n-k} |x_t - \mu||x_{t+k} - \mu|, \tag{6}$$

where  $\mu$  and  $\delta$  are the mean value and the standard deviation of the discrete time series,  $\{x_t\}$ , respectively, we have an expected value to quantify how fast the



(a) The instantaneous amplitude



(b) The auto-correlation function

Fig. 7. (a) The time functions of the instantaneous amplitude of the IMF mode 4 for the normal (solid line) and the mildly demented subjects (gray dashed line). (b) The comparison of the autocorrelation functions of instantaneous amplitude between the normal (right-pointing triangle) and the mildly demented subjects (left-pointing triangle).

instantaneous amplitude changes over time when the signal (i.e. the instantaneous amplitude) looks noisy. The comparison of the instantaneous amplitude autocorrelation function between the normal and the mildly demented subjects are given in Fig. 7(b). Clearly, the correlation for the demented patient decays more quickly, it is below 0.5 at short lag of 20 sample points (i.e. 0.14s), while a high value ( $> 0.8$ ) at the same lag can be kept in the normal subject.

According to the animal studies, the alpha rhythms are generated from the interaction between the cortical neurons and the thalamus, which is considered as the pacemaker neurons.<sup>4</sup> The pacemaker neurons oscillate synchronously in the 7.5–12.5 Hz frequency range.<sup>41</sup> There are many influences regulating the extent and the frequency of thalamic rhythm such as neurotransmitters, neuronal pathways, and different ion-channels. Changes of the balance between these influences in pathological conditions of the brain may manifest as the desynchronization in alpha rhythms. For example, alpha waves are slowed by decreased blood flow in the occipital area.<sup>42</sup> Accordingly, the more integrated these feedback loops between the cortical neuron and the thalamus, the more consistent the alpha rhythms. It is in agreement with our finding that the normal subject can keep each constitutive

alpha wave relative invariant in both frequency (i.e. narrow instantaneous frequency distribution) and in amplitude (i.e. slowly decayed autocorrelation function) over time, while the demented patients have lost this consistency.

## 4.2. *Brain topography*

To function normally, the brain requires good mechanisms for the integration of many brain regions into specialized network for each particular task. Such sophisticated mechanisms of the integration in the human brain may project into many dominant frequency bands, which represent the synchronization of particular groups of the brain waves. It is difficult to describe or examine those integrations only by the traditional line format displays of EEG. Therefore, people have been searching for new methods to probe both temporal and spatial presentation of the electrical activities of the brain.<sup>43</sup> The most important thing is to combine all the channels of the EEG into a topographical map, which may easily present the spatial distribution of the brain activities. Namely, the locations of changes in rhythms, amplitudes, or any derived qEEG parameters (e.g. absolute or relative power in given frequency bands<sup>43,44</sup>) could be shown in a topographical map.

In this study, we provide two EEG topographies which are built based on parameters acquired from the HHT, they are the power of oscillations related to alpha rhythms (see upper panels in Fig. 8) and the correlation index (CI) between the channels (see lower panels in Fig. 8). Since the alpha waves represent the activities of the visual cortex in a state called relaxed awareness, they are posterior dominant in the normal subject as shown in Fig. 8(a), whereas the demented patients have lost this dominance (see Figs. 8(b) and 8(c)). We hypothesize that some mechanisms for the integration of different brain regions to perform certain functions such as wakefulness or cognition are disrupted in the pathological brains.

It is worthy of notice that a highly bilateral symmetry is displayed in the topography of the alpha rhythms in the normal brain (see Fig. 8(a)), whereas the symmetry is lost in both demented patients with different clinical severities. It is generally believed that the loss of symmetry in EEG is pathological.<sup>7</sup>

The EEG coherence plays an important role in the assessment of cortico-cortical connectivity.<sup>45</sup> The coherence between near electrodes is particularly influenced by short connections, while the coherence between distant electrodes is mainly by long axon connections. Using the coherence, we can examine the degree of similarity between two signals. This can be evaluated through the cross-spectrum, given by

$$C(f) = \frac{|S_1(f)S_2^*(f)|^2}{|S_1(f)|^2|S_2(f)|^2}, \quad (7)$$

where  $S_1(f)$  and  $S_2(f)$  are Fourier spectrums for two EEG signals. A coherence value close to 0 indicates weak relationship between these two signals. Such Fourier-based coherence is only valid in stationary condition,<sup>35</sup> nevertheless, in the previous

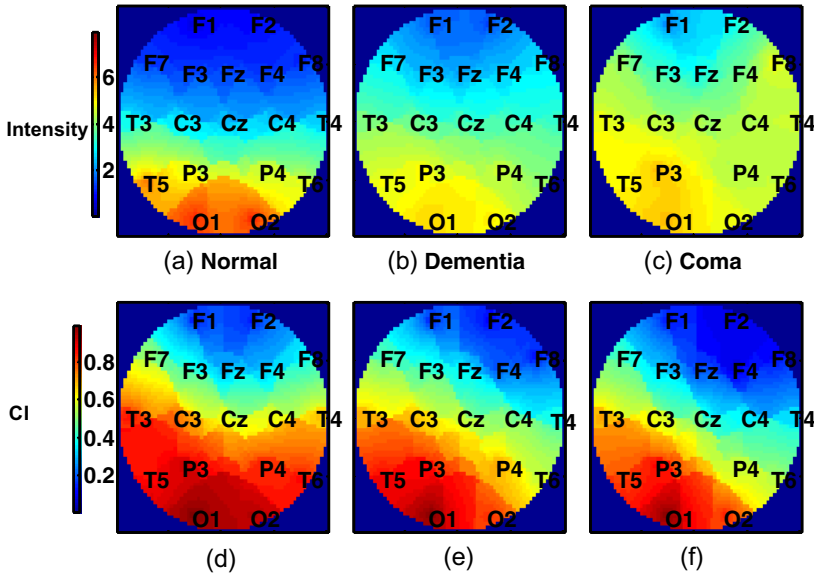


Fig. 8. EEG topographies of the power of oscillations related to alpha rhythm (IMF mode 4) are illustrated in upper panel for the subjects who are (a) normal control (b) mildly demented (c) severe demented in deep coma. The subplots in lower panel demonstrate the EEG topographies of the correlation index (CI) of oscillations related to alpha rhythm (IMF mode 4) between the O1 and the other channels for each subject.

section we have proved that the EEG signals are not stationary. To provide a more precise parameter to characterize the relationship between two signals, the correlation coefficient in time domain is adopted here, given by

$$C_{\text{corr}} = \frac{E[(x_t - \bar{x}_t)(y_t - \bar{y}_t)]}{\sigma_{x_t} \cdot \sigma_{y_t}}, \tag{8}$$

where  $\bar{x}_t$  and  $\bar{y}_t$  are the mean values of the time series,  $x_t$  and  $y_t$  respectively, and  $\sigma_{x_t}$  and  $\sigma_{y_t}$  are the corresponding standard deviations.

Nonstationarity leads the Fourier-based coherence to incorporate unwanted interferences, i.e. the discontinuity in amplitude or instantaneous frequency will induce the windowing effect in time domain, which broadens frequency components (i.e. the resulting frequency response turns out the true spectrum convolved with frequency response of time window). As a consequence, the spectral response of alpha rhythms would not be contributed solely from the waves oscillating within the frequencies of 8–13Hz; the windowing effect makes them blurred by mixing other brain oscillations like theta (4–7.5 Hz), or beta (14–26 Hz) rhythms. According to the simulations in our previous research,<sup>15</sup> EEMD, the HHT-based filter can attenuate nonstationary interferences substantially, and thus the cross correlation of extracted time domain EEG signals by means of EEMD is better to

represent the relationship between two regions. Figure 8(b) demonstrates brain maps of the correlation coefficients between each channel and channel O1, which holds the maximum intensity of alpha rhythms in all the three subjects. Clearly, the correlation becomes weaker with the distance between the two channels, in addition, in the normal subject, the correlation between each channel in the right hemisphere and O1 is very similar to that acquired from channels in left hemisphere, thus the coherence (time domain correlation) shows a bilaterally symmetrical pattern. But this symmetry disappears in the brain maps of both demented patients. EEG coherence has been used as a measure for the synchronization of electrical activities of the neurons.<sup>46</sup> The connection between neurons could be shown by two kinds of coherences, intrahemispheric, and interhemispheric coherences. Anatomically, the tracts for the intrahemispheric electrical conduction are the intrahemispheric cortical–cortical or cortical–subcortical fibers, while the corpus callosum is the tract for the communication between the two hemispheres. The loss of interhemispheric coherences in both demented patients may indicate a failure of the connectivity through the corpus callosum, while the decrease of intrahemispheric coherences is the result of cortical deafferentation from the subcortical structures such as thalamus, the pacemaker of the alpha rhythms. Our study shows that the coherences in the mildly demented patient are of greater values compared to the comatose one. This may suggest that the degree of the loss of brain connectivity could be graded and correlated with the severity of the disease.

In some previous image studies of MRI,<sup>47–51</sup> corpus callosum atrophy is observed in the AD patients and is also severity-related. Because we did not perform MRI to record the thickness of their corpus callosum of these three subjects, whether the loss of intrahemispheric symmetry in our coherence maps resulting from “atrophy of the corpus callosum” needs further studies to clarify.

## 5. Discussion and Remarks

In this study, based on HHT, we propose a novel analysis for the alpha rhythms of EEG, which are of nonlinear and nonstationary physiological data.

The alpha rhythms are one of the dominant frequency components of the electrical activities detected at the surface of the brain. The pacemaker neurons of the alpha rhythms are believed to be distributed throughout the thalamus, which synchronously oscillate in the frequency range of 7.5–12.5 Hz. Physiologically it represents a state called relaxed awareness and is mostly seen at the surface of visual cortex. Decrease of the frequency, the amplitude, bilateral symmetry, and the regularity of the alpha rhythms are expected in aging or pathological degenerations. There are some feedback loops in the brain to control this system, they are loops between brain stem (i.e. the reticular activating system), thalamus, and visual cortex. We suppose these loops modulate at least one of the frequency, the degree of synchronization, or the location of the alpha rhythms.

In the present study, we use HHT analysis to define some features of the alpha rhythms as the followings:

- (i) The stationary analysis based on Hilbert–Huang spectrum identifies the consistent and monotonic alpha rhythms as the dominant oscillations of EEG signal while acquired from the eye-closed normal subject.
- (ii) The existence of intrawave frequency modulation in normal alpha rhythms provides a significant evidence that the process of the generation of the alpha rhythms including oscillatory firing from thalamic neurons and the propagation from thalamus to cortex is nonlinear, and thus it is common to observe the nonlinear waveform distortion in normal alpha rhythms. Such nonlinear process does not alter the cycle length for each wave. In this study, the existence of inconsistent cycle length of alpha rhythms in demented patients may be due to desynchronous firing thalamic neurons. On the other hand, the generation of rhythmical EEG activity is inhibited by the reticular activating systems physiologically. As in eye open conditions, the reticular activating systems are passing influence to the thalamus, the periods or envelope for each constitutive wave in the alpha rhythms cannot keep consistent and as a result, interwave frequency modulations and quickly decayed auto-correlation functions are found. Therefore, we suppose the intrawave frequency modulation represents the alteration of pacemaker firing while the interwave frequency modulation represents the feedback loops inside the brain between the reticular formation, thalamus, and the cortex. The clinical meanings of these modulations need to be specified in individual case, as it could be either physiological or pathological.
- (iii) The brain topography of the alpha rhythms for normal subject shows occipital predominant and bilateral symmetry, which are lost in both demented brain with a dose-response relationship. The topography of the coherences based on HHT seems to provide a more accurate and convenient way to compare the difference between different locations of the brain, which is important in the study of the mechanisms of those networks for different brain functions.

Through out the study, we have been trying to clarify the physiological meanings and behaviors of the alpha rhythms, yet with only three subjects, many questions has left for the future study. For instance, there is a clinical condition called alpha coma, which means the patient is in a comatose state while the EEG shows relatively monotonous and much diffuse topographically.<sup>52</sup> This kind of alpha range rhythms is different from the normal in the unresponsiveness to any sensory input. Therefore, whether oscillations of similar frequency represent the same source is questionable. This leads to our further plan to examine more waves on different frequency bands and in other physiological or pathological conditions.

In conclusion, we have established the differences of alpha rhythms in three different brains by several nonlinear quantitative methods. The EEG is a noninvasive and highly cost-effective clinical tool. Moreover, by using the HHT, the better understanding of the changes of frequencies, amplitudes, and phases is possible in

both time and space domain. Finally, it might empower the studies in psychology, aging, or pathology of the brain.

## Acknowledgments

This study was supported by NSC (Taiwan, ROC), Grant No. 97-2627-B-008-006, and joint foundation of CGH and NCU, Grant No. CNJRF-96CGH-NCU-A3 to M.-T. Lo.

## References

1. B. J. Roach and D. H. Mathalon, Event-related EEG time-frequency analysis: An overview of measures and an analysis of early gamma band phase locking in schizophrenia, *Schizophr. Bull.* **34**(5) (2008) 907–926.
2. D. V. Iosifescu, Prediction of response to antidepressants: Is quantitative EEG (QEEG) an alternative? *CNS Neurosci. Ther.* **14**(4) (2008) 263–265.
3. F. Letemendia and G. Pampiglione, Clinical and electroencephalographic observations in Alzheimer's disease, *J. Neurol. Neurosurg. Psychiatry* **21**(3) (1958) 167–172.
4. W. Klimesch, EEG alpha and theta oscillations reflect cognitive and memory performance: A review and analysis, *Brain Res. Brain Res. Rev.* **29**(2–3) (1999) 169–195.
5. E. B. Gordon, Sim et al., The EEG in presenile dementia, *J. Neurol. Neurosurg. Psychiatry* **30**(3) (1967) 285–291.
6. M. W. Difrancesco, S. K. Holland and J. P. Szaflarski, Simultaneous EEG/functional magnetic resonance imaging at 4 Tesla: Correlates of brain activity to spontaneous alpha rhythm during relaxation, *J. Clin. Neurophysiol.* **25**(5) (2008) 255–264.
7. B. J. Fish, *Fisch and Spehlmann's EEG Primer: Basic Principles of Digital and Analog EEG* (Elsevier, 1999).
8. A. Babloyantz, J. Salazar and C. Nicolis, Evidence of chaotic dynamics of brain activity during the sleep cycle, *Phys. Lett. A* **111**(3) (1985) 152–156.
9. A. Babloyantz and C. Lourenco, Computation with chaos: A paradigm for cortical activity, *Proc. Natl. Acad. Sci. USA* **91**(19) (1994) 9027–9031.
10. A. Babloyantz and A. Destexhe, Low-dimensional chaos in an instance of epilepsy, *Proc. Natl. Acad. Sci. USA* **83**(10) (1986) 3513–3517.
11. P. E. Rapp, I. D. Zimmerman, A. M. Albano et al., Dynamics of spontaneous neural activity in the Simian motor cortex: The dimension of chaotic neurons, *Phys. Lett. A* **110**(6) (1985) 334–338.
12. G. E. P. Box, G. M. Jenlins and G. C. Reinsel, *Time Series Analysis, Forecasting and Control* (Englewood Cliffs, NJ Prentice Hall, 1994).
13. M. F. Schlesinger, Fractal time and 1/f noise in complex systems, *Ann. New York Acad. Sci.* **504** (Persp. Biol. Dynam. Theoret. Med.) (1987) 214–228.
14. L. S. Liebovitch, Testing fractal and Markov models of ion channel kinetics, *Biophys. J.* **55**(2) (1989) 373–377.
15. M. T. Lo, V. Novak, C. K. Peng et al., Assessment of nonlinear phase interaction between nonstationary signals: A comparison study of methods based on Hilbert–Huang and Fourier transforms, *Phys. Rev. E* (2009).
16. N. E. Huang, Z. Shen, S. R. Long et al., The empirical mode decomposition method and the Hilbert spectrum for non-stationary time series analysis, *Proc. Roy. Soc. London A* **454** (1998) 903–995.

17. W. Huang, Z. Shen, N. E. Huang *et al.*, Engineering analysis of biological variables: An example of blood pressure over 1 day, *Proc. Natl. Acad. Sci. USA* **95** (1998) 4816–4821.
18. K. Hu, C. K. Peng, M. Czosnyka *et al.*, Nonlinear assessment of cerebral autoregulation from spontaneous blood pressure and cerebral blood flow fluctuations, *Cardio-vasc. Eng.* **8**(1) (2008) 60–71.
19. M. T. Lo, K. Hu, Y. Liu *et al.*, Multimodal pressure–flow analysis: Application of Hilbert Huang transform in cerebral blood flow regulation, *Eurasip J. Adv. Signal Process.* (2008).
20. K. Hu, M. T. Lo, C. K. Peng *et al.*, Nonlinear pressure–flow relationship is able to detect asymmetry of brain blood circulation associated with midline shift, *J. Neuro-trauma* **26**(2) (2009) 227–233.
21. V. Novak, A. C. Yang, L. Lepicovsky *et al.*, Multimodal pressure–flow method to assess dynamics of cerebral autoregulation in stroke and hypertension, *Biomed. Eng. Online* **3**(1) (2004) 39.
22. K. Hu, C. K. Peng, N. E. Huang *et al.*, Altered phase interactions between spontaneous blood pressure and flow fluctuations in type 2 diabetes mellitus: Nonlinear assessment of cerebral autoregulation, *Phys. A–Stat. Mech. Appl.* **387**(10) (2008) 2279–2292.
23. R. Maestri, G. D. Pinna, A. Accardo *et al.*, Nonlinear indices of heart rate variability in chronic heart failure patients: Redundancy and comparative clinical value, *J. Cardiovasc. Electrophysiol.* **18**(4) (2007) 425–433.
24. R. Balocchi, D. Menicucci, E. Santarcangelo *et al.*, Deriving the respiratory sinus arrhythmia from the heartbeat time series using empirical mode decomposition, *Chaos, Solitons Fractals* **20**(1) (2004) 171–177.
25. C. M. Sweeney-Reed and S. J. Nasuto, A novel approach to the detection of synchronisation in EEG based on empirical mode decomposition, *J. Comput. Neurosci.* **23**(1) (2007) 79–111.
26. M. R. Nuwer, G. Comi, R. Emerson *et al.*, IFCN standards for digital recording of clinical EEG. International Federation of Clinical Neurophysiology, *Electroencephalogr. Clin. Neurophysiol.* **106**(3) (1998) 259–261.
27. Z. Wu and N. E. Huang, Ensemble empirical mode decomposition: A noise-assisted data analysis method, Centre for Ocean-Land-Atmosphere Studies, Tech Rep No 2005; 193.
28. Z. Wu and N. E. Huang, Ensemble empirical mode decomposition: A noise-assisted data analysis method, *Adv. Adapt. Data Anal.* **1** (2009) 1–41.
29. M. G. Rosenblum, A. S. Pikovsky and J. Kurths, Phase synchronization of chaotic oscillators, *Phys. Rev. Lett.* **76**(11) (1996) 1804–1807.
30. P. Tass, M. G. Rosenblum, J. Weule *et al.*, Detection of  $n : m$  phase locking from noisy data: Application to magnetoencephalography, *Phys. Rev. Lett.* **81**(15) (1998) 3291–3299.
31. C. Schafer, M. G. Rosenblum, J. Kurths *et al.*, Heartbeat synchronized with ventilation, *Nature* **392**(6673) (1998) 239–240.
32. N. Delprat, B. Escudie, P. Guillemain *et al.*, Asymptotic wavelet and Gabor analysis — extraction of instantaneous frequencies, *IEEE Trans. Inform. Theory* **38**(2) (1992) 644–664.
33. D. B. Lindsley, Psychological phenomenon and the electroencephalogram, *Electroencephalogr. Clin. Neurophysiol.* **4**(4) (1952) 443–456.
34. S. Tong, Z. Li, Y. Zhu *et al.*, Describing the nonstationarity level of neurological signals based on quantifications of time–frequency representation, *IEEE Trans. Biomed. Eng.* **54**(10) (2007) 1780–1785.

35. S. N. Prabhakar, *Modern Spectrum Analysis of Time Series* (CRC Press, Boca Raton, 1996).
36. V. L. Newhouse, E. S. Furgason and G. F. Johnson *et al.*, The dependence of ultrasound doppler bandwidth on beam geometry, *IEEE Trans. Sonics Ultrason.* **27**(2) (1980) 50–59.
37. D. W. Liddell, Investigations of EEG findings in presenile dementia, *J. Neurol. Neurosurg. Psychiatry* **21**(3) (1958) 173–176.
38. H. Soinenen, V. J. Partanen, E. L. Helkala *et al.*, EEG findings in senile dementia and normal aging, *Acta Neurol. Scand.* **65**(1) (1982) 59–70.
39. R. P. Brenner, C. F. Reynolds III, R. F. Ulrich, Diagnostic efficacy of computerized spectral versus visual EEG analysis in elderly normal, demented and depressed subjects, *Electroencephalogr. Clin. Neurophysiol.* **69**(2) (1988) 110–117.
40. Y. Fischer, B. H. Gahwiler and S. M. Thompson, Activation of intrinsic hippocampal theta oscillations by acetylcholine in rat septo-hippocampal cocultures, *J. Physiol.* **519**(2) (1999) 405–413.
41. E. R. John, The neurophysics of consciousness, *Brain Res. Brain Res. Rev.* **39**(1) (2002) 1–28.
42. I. A. Sulg, S. Cronqvist, H. Schuller *et al.*, The effect of intracardial pacemaker therapy on cerebral blood flow and electroencephalogram in patients with complete atrioventricular block, *Circulation* **39** (1969) 487–494.
43. M. R. Nuwer, Quantitative EEG: I. Techniques and problems of frequency analysis and topographic mapping, *J. Clin. Neurophysiol.* **5**(1) (1988) 1–43.
44. A. F. Leuchter, I. A. Cook, R. B. Lufkin *et al.*, Cordance: A new method for assessment of cerebral perfusion and metabolism using quantitative electroencephalography, *Neuroimage* **1**(3) (1994) 208–219.
45. R. W. Thatcher, P. J. Krause and M. Hrybyk, Cortico-cortical associations and EEG coherence: A two-compartmental model, *Electroencephalogr. Clin. Neurophysiol.* **64**(2) (1986) 123–143.
46. G. Pfurtscheller and C. Andrew, Event-related changes of band power and coherence: Methodology and interpretation, *J. Clin. Neurophysiol.* **16**(6) (1999) 512–519.
47. S. J. Teipel, W. Bayer, G. E. Alexander *et al.*, Regional pattern of hippocampus and corpus callosum atrophy in Alzheimer's disease in relation to dementia severity: Evidence for early neocortical degeneration, *Neurobiol. Aging* **24**(1) (2003) 85–94.
48. S. J. Teipel, W. Bayer, G. E. Alexander *et al.*, Progression of corpus callosum atrophy in Alzheimer disease, *Arch Neurol.* **59**(2) (2002) 243–248.
49. S. J. Teipel, H. Hampel, G. E. Alexander *et al.*, Dissociation between corpus callosum atrophy and white matter pathology in Alzheimer's disease, *Neurology* **51**(5) (1998) 1381–1385.
50. H. Hampel, S. J. Teipel, G. E. Alexander *et al.*, Corpus callosum atrophy is a possible indicator of region- and cell type-specific neuronal degeneration in Alzheimer disease: A magnetic resonance imaging analysis, *Arch Neurol.* **55**(2) (1998) 193–198.
51. P. Vermersch, J. Roche, M. Hamon *et al.*, White matter magnetic resonance imaging hyperintensity in Alzheimer's disease: Correlations with corpus callosum atrophy, *J. Neurol.* **243**(3) (1996) 231–234.
52. A. M. Husain, Electroencephalographic assessment of coma, *J. Clin. Neurophysiol.* **23**(3) (2006) 208–220.